

# ChemComm

Accepted Manuscript



This is an *Accepted Manuscript*, which has been through the Royal Society of Chemistry peer review process and has been accepted for publication.

*Accepted Manuscripts* are published online shortly after acceptance, before technical editing, formatting and proof reading. Using this free service, authors can make their results available to the community, in citable form, before we publish the edited article. We will replace this *Accepted Manuscript* with the edited and formatted *Advance Article* as soon as it is available.

You can find more information about *Accepted Manuscripts* in the [Information for Authors](#).

Please note that technical editing may introduce minor changes to the text and/or graphics, which may alter content. The journal's standard [Terms & Conditions](#) and the [Ethical guidelines](#) still apply. In no event shall the Royal Society of Chemistry be held responsible for any errors or omissions in this *Accepted Manuscript* or any consequences arising from the use of any information it contains.

## COMMUNICATION

# Proton reduction by molecular catalysts in water under demanding atmospheres

Cite this: DOI: 10.1039/x0xx00000x

David W. Wakerley,<sup>a</sup> Manuela A. Gross<sup>a</sup> and Erwin Reisner<sup>a\*</sup>Received 06th August 2014,  
Accepted xxth xx 20xx

DOI: 10.1039/x0xx00000x

www.rsc.org/

The electrocatalytic proton reduction activity of a Ni bis(diphosphine) (NiP) and a cobaloxime (CoP) catalyst has been studied in water in the presence of the gaseous inhibitors O<sub>2</sub> and CO. CoP shows an appreciable tolerance towards O<sub>2</sub>, suffering only slightly from competing O<sub>2</sub> reduction. In contrast, NiP is strongly inhibited by O<sub>2</sub>, but produces H<sub>2</sub> under high CO concentrations.

The realisation of an artificial photosynthetic system would offer a sustainable route to clean and storable energy.<sup>1</sup> This process could generate H<sub>2</sub> fuel, or a gas mixture of H<sub>2</sub> and CO, known as syngas, which can be used to produce long-chain hydrocarbons or methanol.<sup>2</sup> Proton reduction catalysts are an integral part of either system and have consequently generated considerable research interest.<sup>3</sup>

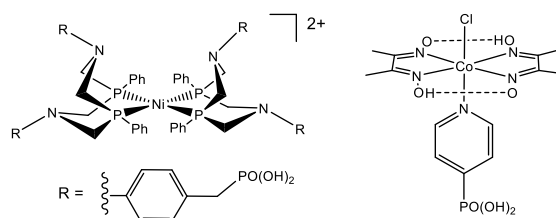
Inhibitor tolerance under real-world operating conditions is a vital trait for a proton reduction catalyst, but has received relatively little attention to date. Depending on the intended use of a system, proton reduction catalysts could be exposed to large amounts of O<sub>2</sub> (water splitting) or CO (CO<sub>2</sub> splitting). Trace amounts of such inhibitors typically poison the most active H<sub>2</sub> evolution catalysts, such as platinum<sup>4</sup> and H<sub>2</sub>-producing enzymes (hydrogenases).<sup>5,6</sup>

Molecular synthetic catalysts offer an alternative route to proton reduction<sup>7–9</sup> and it has recently emerged that some molecular catalysts are tolerant towards O<sub>2</sub> in aqueous solution. This observation has prompted a number of contemporary studies into H<sub>2</sub> evolution under aerobic conditions. Co-based complexes make up the majority of these O<sub>2</sub> tolerant species; cobaloximes were the first earth-abundant catalysts shown to be functional under air,<sup>10</sup> followed by a Co-corrole catalyst<sup>11</sup> and a Co-microperoxidase.<sup>12</sup>

Recently, a rationally designed bis(1,5-R'-diphospha-3,7-R''-diazacyclooctane)Ni catalyst from DuBois and co-workers has set a new benchmark for H<sub>2</sub> production activity.<sup>13</sup> Derivatives of this Ni catalyst have since been able to generate considerable amounts of H<sub>2</sub> from aqueous solutions,<sup>14,15</sup> an important step in the development of

water-splitting systems.<sup>16</sup> However, inhibition remains completely unexplored for this promising type of catalyst.

Herein, we have used a water-soluble Ni bis(diphosphine) catalyst (NiP),<sup>14</sup> as well as a cobaloxime (CoP)<sup>17</sup> (Scheme 1) to study inhibition of catalytic proton reduction activity by O<sub>2</sub> and CO. Inhibition prevents catalysts from undergoing redox reactions essential for catalytic H<sub>2</sub> evolution, therefore electrochemical analysis was fundamental to this work. Cyclic voltammetry has been used to monitor changes in the redox and electrocatalytic activity of CoP and NiP under atmospheres of O<sub>2</sub> or CO on a short time-scale and controlled potential electrolysis (CPE) combined with H<sub>2</sub> analysis has explored the inhibition of H<sub>2</sub>-evolution activity over longer periods of time. Spectroelectrochemistry allowed the potential-dependent formation of inhibited species to be analysed.



**Scheme 1.** Chemical structure of Ni and Co catalysts used in this study. Both compounds contain phosphonic acid moieties to allow dissolution in aqueous media and the Ni and Co catalysts have therefore been labelled as NiP and CoP, respectively.

Cyclic voltammograms (CVs) were recorded on a glassy carbon disk electrode (0.07 cm<sup>2</sup>) at 100 mV s<sup>-1</sup> using conditions optimised for high catalyst activity (pH 4.5 for NiP<sup>14</sup> and pH 7 for CoP<sup>17,18</sup>). Initial studies into H<sub>2</sub> inhibition (up to 100% H<sub>2</sub>) showed no product inhibition for NiP and CoP (Figure S1), allowing the effect of other inhibiting gases to be established during proton reduction. Figures 1a and b display CVs of NiP and CoP under inert and aerobic atmospheres. Irreversible O<sub>2</sub> reduction occurs at E<sub>p</sub> = -0.5 V vs. normal hydrogen electrode (NHE) at the glassy carbon electrode,

resulting in an increased current response in air, which must be taken into account in this analysis.

Under inert conditions, the CV of **NiP** displays two waves at potentials more negative than  $-0.3$  V vs. NHE, which have been assigned to the reduction of  $\text{Ni}^{\text{II}}$  to  $\text{Ni}^{\text{I}}$  followed by  $\text{Ni}^{\text{I}}$  to a formal  $\text{Ni}^{\text{0}}$ .<sup>14</sup> The CV lacks a strong catalytic wave, presumably because most of the proton reduction by **NiP** occurs after  $\text{Ni}^{\text{0}}$  has diffused away from the electrode-solution interface.<sup>19</sup> The CV trace recorded under 21%  $\text{O}_2$  (blue trace in Figure 1a) shows almost no change compared to inert conditions when the  $\text{O}_2$  reduction current (gray trace) is disregarded. The degree of inhibition could not be obtained from the CVs due to the weak catalytic wave of **NiP**. CPE subsequently confirmed the catalytic proton reduction activity of **NiP** and was used to monitor the degree of  $\text{O}_2$  inhibition (see below).

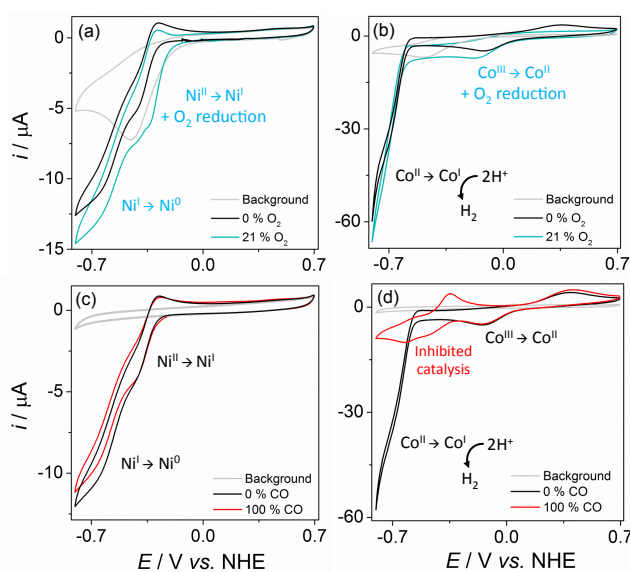


**Figure 1.** CVs ( $100 \text{ mV s}^{-1}$  on a glassy carbon disk electrode) of (a) and (c) **NiP** (1 mM) in citrate buffer (0.1 M, pH 4.5) and (b) and (d) **CoP** (1 mM) in triethanolamine/ $\text{Na}_2\text{SO}_4$  (0.1 M each, pH 7) in atmospheres of 100%  $\text{N}_2$ , 21%  $\text{O}_2$  (air) and 100% CO. The gray background traces were generated from air or CO saturated electrolyte solutions without catalyst.

The analogous CVs of **CoP** are displayed in Figure 1b. Under inert conditions, the cobaloxime first undergoes a reduction from  $\text{Co}^{\text{III}}$  to  $\text{Co}^{\text{II}}$ , followed by a strong catalytic wave at an onset potential of  $-0.6$  V, as  $\text{Co}^{\text{II}}$  is reduced to  $\text{Co}^{\text{I}}$  and proton reduction catalysis is initiated.<sup>20</sup> Under 21%  $\text{O}_2$ , the proton reduction wave of **CoP** is almost identical suggesting high catalytic activity under air. The  $\text{O}_2$  reduction wave at  $-0.5$  V however overlaps with the  $\text{Co}^{\text{III}}/\text{Co}^{\text{II}}$  reduction wave around  $-0.2$  V vs. NHE suggesting that  $\text{Co}^{\text{II}}$  may be reducing dissolved  $\text{O}_2$ . Catalytic  $\text{H}_2$  generation is thus in competition with oxidation of the reduced Co species ( $\text{Co}^{\text{II}}$  and  $\text{Co}^{\text{I}}$ ) by  $\text{O}_2$ . This was confirmed through analysis of the  $\text{Co}^{\text{III}}/\text{Co}^{\text{II}}$  redox couple in air, which showed a loss of the anodic  $\text{Co}^{\text{II}}$  to  $\text{Co}^{\text{III}}$  wave due to prior oxidation of  $\text{Co}^{\text{II}}$  by  $\text{O}_2$  (Figure S2).<sup>21,22</sup>

CVs of **NiP** and **CoP** under a CO atmosphere are presented in Figures 1c and d. Assuming saturation of water with CO at a concentration of 1 mM,<sup>23</sup> the concentration of CO is comparable to the catalyst concentration. The reduction waves of **NiP** do not show any significant changes upon introduction of 100% CO (Figure 1c).

The cobaloxime demonstrates a low tolerance towards CO compared to the Ni bis(diphosphine) catalyst (see results from CPE below). CVs of **CoP** under  $\text{N}_2$  and CO have identical  $\text{Co}^{\text{III}}/\text{Co}^{\text{II}}$  reduction ( $E_p = -0.14$  V) and oxidation ( $E_p = +0.4$  V) waves under  $\text{N}_2$  and CO (Figure 1d). Upon reduction of  $\text{Co}^{\text{II}}$  to  $\text{Co}^{\text{I}}$  however, the proton reduction activity is no longer observed as the cobaloxime is inhibited.

A long-term, more quantitative measure of inhibition was achieved through CPE, which analysed changes in the  $\text{H}_2$  produced by both catalysts. CPE was particularly important for the study of **NiP**, where little catalysis was observed in the CVs. A glassy carbon rod (approximately  $2 \text{ cm}^2$ ) was held at  $-0.4$  V vs. NHE for **NiP** and  $-0.7$  V vs. NHE for **CoP**, whilst stirring under different atmospheres. The  $\text{H}_2$  produced was detected by headspace gas chromatography (Figure 2 and Table S1). Faradaic efficiencies were calculated and gave respectable numbers for molecular catalysts held at such low overpotentials ( $> 65\%$  in all cases).

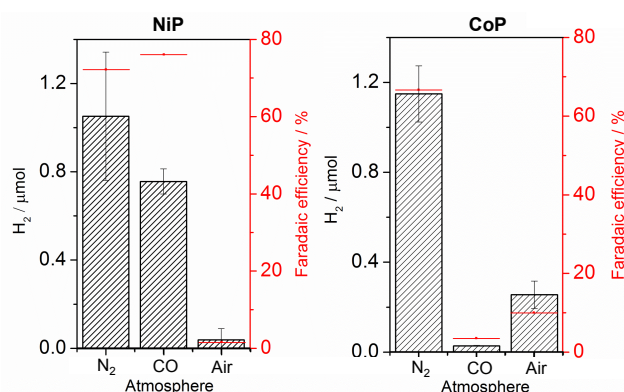


**Figure 2.** Electrocatalytic production of  $\text{H}_2$  (black bars) and Faradaic efficiency (red lines) from CPE of (a) **NiP** (0.5 mM) in citrate buffer (0.1 M, pH 4.5) at  $-0.4$  V vs. NHE for 60 min and (b) **CoP** (0.5 mM) in triethanolamine/ $\text{Na}_2\text{SO}_4$  (0.1 M each, pH 7) at  $-0.7$  V vs. NHE for 15 min.

CPE of **CoP** for 15 min in the presence of air illustrated the tolerance of cobaloximes to  $\text{O}_2$ . The CPE timescale was kept short to avoid the formation of heterogeneous catalysts on the electrode surface.<sup>24</sup> A drop in proton reduction activity was seen under air compared to  $\text{N}_2$ , due to increasing catalyst oxidation by  $\text{O}_2$ , yet the catalyst still retained appreciable activity. The Faradaic efficiency similarly drops due to increasing  $\text{O}_2$  reduction by both the electrode and catalyst. The remarkable tolerance towards  $\text{O}_2$  has been attributed previously to the abundance of aqueous protons over  $\text{O}_2$  in the electrochemical cell<sup>10</sup> ( $0.3 \text{ mM O}_2$  under aerobic conditions) combined with the low affinity of the cobaloxime for forming irreversible inhibition products with  $\text{O}_2$ . The reduction of oxygen presumably leads to the production of water in a similar manner to oxygen tolerant hydrogenases,<sup>25</sup> allowing parallels to be drawn between these systems.

The activity of **NiP** was much more sensitive to  $\text{O}_2$ . Despite the apparent tolerance displayed in the CV (Figure 1a), 60 min of CPE under air at  $-0.4$  V vs. NHE produced only negligible amounts of  $\text{H}_2$ . The level of  $\text{H}_2$  recorded was comparable to the small quantity produced by the glassy carbon rod electrode without a catalyst. This complete inhibition of **NiP** suggests that an oxidised, inactive inhibition product is forming. Studies into  $\text{O}_2$  reduction by similar

structures identified the formation of inactive phosphine oxides at low Ni oxidation states<sup>26</sup> and gives a possible explanation for the observed inhibition on the CPE timescale. It may thus be concluded that in order to prevent O<sub>2</sub> inhibition it is important to avoid ligand functionality that is susceptible to irreversible oxidation, such as phosphines. Upon repurging with N<sub>2</sub> 72% of the initial H<sub>2</sub> production rate was observed, as the catalyst molecules that are not reduced during CPE are relatively O<sub>2</sub> stable in the bulk solution.

On the other hand, **NiP** is completely tolerant to CO. CPE produced similar levels of H<sub>2</sub> under both 100% CO and 100% N<sub>2</sub> (Figure 2a). The tolerance of **NiP** towards CO is remarkable considering the strongly inhibitive effect of CO on most catalytic surfaces, such as Pt. Experiments into Pt inhibition showed that the H<sub>2</sub> produced by a Pt disk electrode held at -0.4 V vs. NHE for 15 min produced minimal H<sub>2</sub> under CO (Figure S3 and Table S2). The Ni diphosphine structure is designed to mimic hydrogenase enzymes<sup>27</sup> and the coordination sphere of a similar Ni bis(diphosphine) complex has previously demonstrated rapid reversible CO binding.<sup>28</sup> This may prevent the CO from having a significant inhibiting impact on proton reduction in a manner much akin to the few reported CO-tolerant hydrogenases.<sup>29,30</sup>

This result is in contrast to **CoP**, which exposes an easily accessible coordination site in its catalytic cycle,<sup>31</sup> and is consequently susceptible to CO binding. **CoP** was completely inhibited by CO; 15 min of CPE at -0.7 V vs. NHE produced minimal H<sub>2</sub>. However, CO inhibition of **CoP** was completely reversible and 100% of the electroactivity could be regained after purging with N<sub>2</sub> (see Figure S4). The inhibition of the aforementioned Pt disk was irreversible and could not be reactivated with a N<sub>2</sub> purge (Figure S3).

IR-spectroelectrochemical studies were carried out to gain a better understanding of cobaloxime inhibition. Using a spectrochemical cell (Pt working and counter electrodes, Ag wire reference)<sup>32</sup> IR-spectra were taken of [CoCl(dimethylglyoximate)<sub>2</sub>(4-methoxypyridine)] under CO at a range of potentials (Figure 3a). The methoxypyridine analogue of **CoP** was used due to its higher solubility in MeOH.<sup>31</sup> UV-visible spectra were recorded to follow the oxidation state change of the complex (Figure 3b).

Upon reaching potentials at which Co<sup>I</sup> forms in the UV/visible spectra<sup>33</sup> (-0.65 V vs. Ag/Ag<sup>+</sup>) a peak is observed in the IR spectra at 1970 cm<sup>-1</sup>, which is the expected region for a cobaloxime-carbonyl species.<sup>34</sup> This peak has been assigned to substitution of a labile axial ligand at the low Co oxidation state.<sup>35</sup> No carbonyl peak was observed under an atmosphere of N<sub>2</sub> (Figure S5). Electron withdrawing axial ligands, such as CO, decrease cobaloxime proton reduction activity by reducing the basicity of the intermediate Co-H that forms in the catalytic cycle,<sup>31</sup> thereby explaining the loss of catalytic activity.

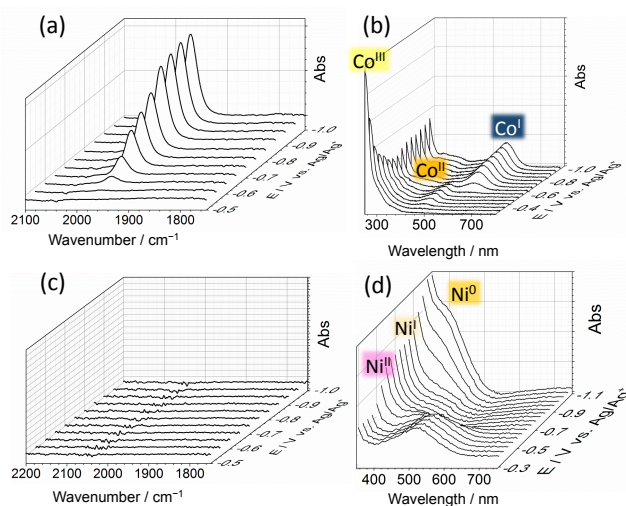


**Figure 3.** (a) and (c) IR-spectroelectrochemical traces of [CoCl(dimethylglyoximate)<sub>2</sub>(4-methoxypyridine)] (~5 mM) and **NiP** (1.25 mM). (b) and (d) UV-visible spectroelectrochemical traces of [CoCl(dimethylglyoximate)<sub>2</sub>(4-methoxypyridine)] (0.25 mM) and **NiP** (0.25 mM). All spectra were taken in the presence of tetrabutylammonium bromide (0.3 M) in MeOH under an atmosphere of CO at increasingly negative potentials.

No Ni-carbonyl peaks are present in the IR spectra of **NiP** under a CO atmosphere at any potential applied (Figure 3c). The UV-visible spectroelectrochemistry displays bands that have been assigned to Ni<sup>II</sup>/Ni<sup>I</sup>/Ni<sup>0</sup> from -0.4 to -1 V vs. Ag/Ag<sup>+</sup> (Figure 3d). The Ni<sup>II</sup> state has a band at 520 nm corresponding to a pink color that is lost upon formation of Ni<sup>I</sup>. The Ni<sup>I</sup> state shows little absorption in the visible region but a shift in the UV peak at 250 nm occurs (Figure S6). Upon formation of Ni<sup>0</sup> a yellow color is seen as suggested by the shoulder in the UV-vis spectrum at 400 nm and previous accounts.<sup>36</sup> The lack of Ni-carbonyl peak across these oxidation states illustrates the tolerance of the Ni bis(diphosphine) to carbonyl binding and explains the sustained proton reduction activity under these conditions.

In summary, Ni bis(diphosphine) and cobaloxime catalysts are widely used state-of-the-art catalysts for the reduction of aqueous protons. Our study demonstrates their distinct tolerance to well-known gaseous inhibitors and illustrates the ways in which molecular catalysts can be designed to fulfill the requirements of a specific system. **NiP** shows unprecedented activity under CO and can therefore be employed in systems where CO is present, such as syngas generating devices. CO reversibly inhibits **CoP** due to the formation of an inactive Co-CO species as confirmed by IR-spectroelectrochemistry. On the other hand, the cobaloxime showed appreciable tolerance towards O<sub>2</sub>, whereas the Ni bis(diphosphine) complex lost all activity. Ongoing studies seek to gain a more detailed understanding of the relationship between the structure of a catalyst and its resultant tolerance to inhibition.

## Notes and references

<sup>a</sup>Christian Doppler Laboratory for Sustainable SynGas Chemistry, Department of Chemistry, University of Cambridge, Lensfield Road, Cambridge CB2 1EW, U.K.



Electronic Supplementary Information (ESI) available: Experimental Details, Supporting Tables S1-S2 and Figures S1-S6. See DOI: 10.1039/c000000x/

1. N. S. Lewis and D. G. Nocera, *Proc. Natl. Acad. Sci. U.S.A.*, 2006, **103**, 15729–15735.
2. M. E. Dry, *Catal. Today*, 2002, **71**, 227–241.
3. P. Du and R. Eisenberg, *Energy Environ. Sci.*, 2012, **5**, 6012–6021.
4. N. P. Dasgupta, C. Liu, S. Andrews, F. B. Prinz, and P. Yang, *J. Am. Chem. Soc.*, 2013, **135**, 12932–12935.
5. E. Reisner, *Eur. J. Inorg. Chem.*, 2011, 1005–1016.
6. F. A. Armstrong, N. A. Belsey, J. A. Cracknell, G. Goldet, A. Parkin, E. Reisner, K. A. Vincent, and A. F. Wait, *Chem. Soc. Rev.*, 2009, **38**, 36–51.
7. T. S. Teets and D. G. Nocera, *Chem. Commun.*, 2011, **47**, 9268–9274.
8. W. T. Eckenhoff and R. Eisenberg, *Dalton Trans.*, 2012, **41**, 13004–13021.
9. H. I. Karunadasa, E. Montalvo, Y. Sun, M. Majda, J. R. Long, and C. J. Chang, *Science*, 2012, **335**, 698–702.
10. F. Lakadamyali, M. Kato, N. M. Muresan, and E. Reisner, *Angew. Chem. Int. Ed.*, 2012, **51**, 9381–9384.
11. B. Mondal, K. Sengupta, A. Rana, A. Mahammed, M. Botoshansky, S. G. Dey, Z. Gross, and A. Dey, *Inorg. Chem.*, 2013, **52**, 3381–3387.
12. J. G. Kleingardner, B. Kandemir, and K. L. Bren, *J. Am. Chem. Soc.*, 2014, **136**, 4–7.
13. M. L. Helm, M. P. Stewart, R. M. Bullock, M. Rakowski DuBois, and D. L. DuBois, *Science*, 2011, **333**, 863–866.
14. M. A. Gross, A. Reynal, J. R. Durrant, and E. Reisner, *J. Am. Chem. Soc.*, 2014, **136**, 356–366.
15. A. Dutta, S. Lense, J. Hou, M. H. Engelhard, J. A. S. Roberts, and W. J. Shaw, *J. Am. Chem. Soc.*, 2013, **135**, 18490–18496.
16. J. R. McKone, N. S. Lewis, and H. B. Gray, *Chem. Mater.*, 2013, **26**, 407–414.
17. F. Lakadamyali and E. Reisner, *Chem. Commun.*, 2011, **47**, 1695–1697.
18. P. Du, K. Knowles, and R. Eisenberg, *J. Am. Chem. Soc.*, 2008, **130**, 12576–12577.
19. C. Costentin, S. Drouet, M. Robert, and J.-M. Savéant, *J. Am. Chem. Soc.*, 2012, **134**, 11235–11242.
20. J. L. Dempsey, B. S. Brunschwig, J. R. Winkler, and H. B. Gray, *Acc. Chem. Res.*, 2009, **42**, 1995–2004.
21. M. Shamsipur, A. Salimi, H. Haddadzadeh, and M. F. Mousavi, *J. Electroanal. Chem.*, 2001, **517**, 37–44.
22. G. N. Schrauzer, *Angew. Chem. Int. Ed.*, 1976, **15**, 417–426.
23. P. Scharlin, R. Battino, E. Silla, I. Tuñón, and J. L. Pascual-Ahuir, *Pure Appl. Chem.*, 1998, **70**, 1895–1904.
24. S. Cobo, J. Heidkamp, P.-A. Jacques, J. Fize, V. Fourmond, L. Guetaz, B. Jusselme, V. Ivanova, H. Dau, S. Palacin, M. Fontecave, and V. Artero, *Nat. Mater.*, 2012, **11**, 802–807.
25. W. Lubitz, H. Ogata, O. Rüdiger, and E. Reijerse, *Chem. Rev.*, 2014, **114**, 4081–4148.
26. J. Y. Yang, R. M. Bullock, W. G. Dougherty, W. S. Kassel, B. Twamley, D. L. DuBois, and M. Rakowski DuBois, *Dalton Trans.*, 2010, **39**, 3001–3010.
27. A. D. Wilson, R. H. Newell, M. J. McNevin, J. T. Muckerman, M. Rakowski DuBois, and D. L. DuBois, *J. Am. Chem. Soc.*, 2006, **128**, 358–366.
28. A. D. Wilson, K. Frazee, B. Twamley, S. M. Miller, D. L. DuBois, and M. Rakowski DuBois, *J. Am. Chem. Soc.*, 2008, **130**, 1061–1068.
29. K. A. Vincent, J. A. Cracknell, O. Lenz, I. Zebger, B. Friedrich, and F. A. Armstrong, *Proc. Natl. Acad. Sci. U.S.A.*, 2005, **102**, 16951–16954.
30. X. Luo, M. Brugna, P. Tron-Infossi, M. T. Giudici-Ortoni, and É. Lojou, *J. Biol. Inorg. Chem.*, 2009, **14**, 1275–1288.
31. D. Wakerley and E. Reisner, *Phys. Chem. Chem. Phys.*, 2014, **16**, 5739–5746.
32. M. Krejčík, M. Daněk, and F. Hartl, *J. Electroanal. Chem.*, 1991, **317**, 179–187.
33. N. M. Muresan, J. Willkomm, D. Mersch, Y. Vaynzof, and E. Reisner, *Angew. Chem. Int. Ed.*, 2012, **51**, 12749–12753.
34. X. Hu, B. M. Cossairt, B. S. Brunschwig, N. S. Lewis, and J. C. Peters, *Chem. Commun.*, 2005, 4723–4725.
35. T. M. McCormick, Z. Han, D. J. Weinberg, W. W. Brennessel, P. L. Holland, and R. Eisenberg, *Inorg. Chem.*, 2011, **50**, 10660–10666.
36. E. S. Wiedner, J. Y. Yang, S. Chen, S. Raugei, W. G. Dougherty, W. S. Kassel, M. L. Helm, R. M. Bullock, M. Rakowski DuBois, and D. L. DuBois, *Organometallics*, 2011, **31**, 144–156.